Proceedings of the International Association for Shell and Spatial Structures (IASS) Symposium 2009, Valencia
Evolution and Trends in Design, Analysis and Construction of Shell and Spatial Structures
28 September – 2 October 2009, Universidad Politecnica de Valencia, Spain
Alberto DOMINGO and Carlos LAZARO (eds.)

Efficiency of thin-walled bars analyses by analytical or numerical methods in the light of experiments

Jan B. OBRĘBSKI*

*Warsaw University of Technology, Faculty of Civil Engineering
00-637 Warsaw, Al. Armii Ludowej 16
Email: jobrebski@poczta.onet.pl

Abstract

Thin-walled bars are widely applied in various structures. In civil engineering they are used for: bridges or viaducts as large span decks, pylons or tall supports and for buildings as carrying columns, girders, elements of roofing or skeletons systems. There, as materials are applied: steel, aluminium, timber, reinforced concrete and various composites. In many papers and dissertations, are observed significant errors by application of particular analyses of such objects. Therefore, paper present results of complex parallel comparative scientific investigations, led by analytical, numerical, hybrid and experimental methods.

Keywords: Thin-walled, bars, analytical-, numerical-, experimental methods, comparisons

1. Introduction

The paper presents mainly some results, diagrams and photos of experiments performed in the years 1988-1992 and elaborated partially a little later. Some observations concerning the phenomena have been quoted in the books [9, 13]. The latest materials have not been published so far. Three kinds of own experiments were performed: for cantilevers with rectangular cross-section (**CS**) oriented vertically (10 bars with Urbaniak (9 papers – e.g. [10,17])) or horizontally (4 bars with Flont [1]); for simple frames composed of two bars (type L) or three bars (type T or Y – with Jankowska [2]) having similar rectangular open **CS**s; or influence of bimoment on similar bars (with Awadi, e.g. [10]). In all above tasks, were observed significant differences between analyses and experimental reality.

The paper is focused on series of 10 brazen cantilevers with rectangular **CS**s of open or closed type, oriented vertically (Figure 1). On one end they were at all fixed and on the second at all free or planarly constrained (mounted rigid steel frame). There, were measured for some steps of growing up loading: displacements and strains by electro-resistance method in two **CS**s. In four cases, the experiments were led to breaking of cantilever (capacity). The results of electro-resistance measurements for 10 bars with vertically oriented **CS**s, were compared with obtained by FEM or by theory of thin-walled bars (**TWB**) supported by own programs or by MS Excel. In last cases, were used for calculation of internal forces closed theoretical formulae or even FDM. The comparisons concern: displacements, strains, normal and shearing stresses, principal stresses with its inclination, angle of non-dilatation strain, character of proper diagrams, etc. The paper provides comparisons, some significant differences, comments and recommendations.

2. Short review of the methods for analyses of thin-walled bars

The literature of **TWB**s is very wide. There, should be mentioned some more significant books: Vlasov's [19] (1940,59), Rutecki [18] (1957), Mutermilch & Kociołek [7] (1964, 72), Kollbrunner & Hajdin [4] (1975), Murray [6] (1984), Obrębski [8,9,13] (1989,91,97), Magnucki & Szyc [5] (1997) and many others (see [9]). So, it was high necessity to recognise real behaviour of **TWB**s and to evaluate assumptions of numerous theories. The main purpose of this paper is to show some observations concerning the effects generated by an internal force called bimoment. As it is well known from literature, warping stresses dependent on the bimoment can reach significant values e.g. up to 50% of stresses from bending moments, Obrębski [9] or even 270% (Smith & Coul – Tall building struct. 1991). Therefore, author from years investigate just foundations of theory for **TWB**s.

3. Investigated bars

To comparative analyses, including experiments, were used large brazen models. They are of three types: cantilevers – for bending-torsion loadings (Figures 1,2,5,6), short bar for loading by pure bimoment (Figures 7,8) and simple frames (Figures 9,11). All these models were having rectangular **CS**s with approximate dimensions 10×20cm.

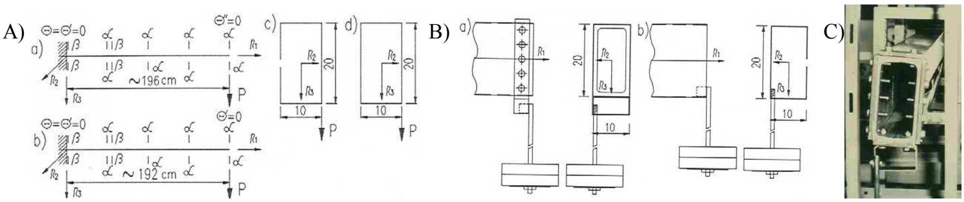

Figure 1: Scheme of the cantilevers A); loading system for **TWB**s with rectangular **C**Ss: open $A)_{c)}$, closed $A)_{d)}$; free end $A)_{a)}$, $B)_{b)}$; planarly constrained displacements $A)_{b)}$, $B)_{a)}$, C).

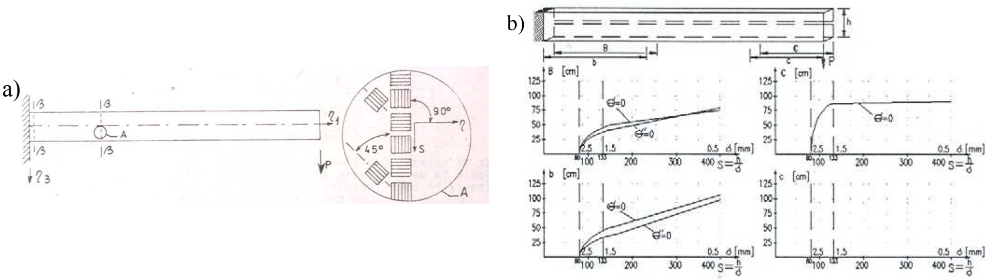

Figure 2: Allocation of electro-resistance tissue (paper) sensors (detail A) [17] a); zones of observed waves on surface of cantilevers

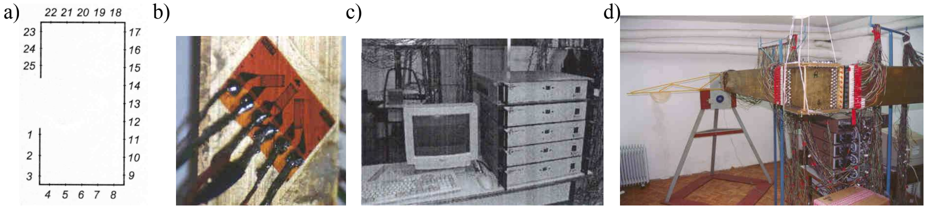

Figure 3: Allocation of foil electro-resistance rosettes in bars **CS** a); rosette with measuring base 3mm b); computer and five scanners c); frame type L and loading system d) [2]

4. Elements of applied theory

Bimoment B is defined according to the theory of **TWB**s in three ways [3,7-9,13,18,19]:

$$B = -\overline{E}\overline{I}_{\hat{\omega}}\Theta'' \quad , \qquad B = \oint \sigma_1 \hat{\omega}\, d\overline{A} \quad , \qquad B = \sum_i P_i \hat{\omega}_i \ , \qquad (1)$$

where: $\overline{E}\overline{I}_{\hat{\omega}}$ - torsion bar rigidity, Θ - torsion angle of bar axis (of the shearing centre), σ_1 - normal longitudinal stresses, $\hat{\omega}$ - generalized sectorial coordinate (warping function) of σ_1 or force P_i position, $\overline{dA} = (E_1 / \overline{E})dA$ reduced elementary area of **CS** [8,9,13]. Moreover, bending-torsion moment as the main part of bar torsion moment is defined as:

$$M_{\hat{\omega}} = -\overline{E}\overline{I}_{\hat{\omega}}\Theta''' , \qquad M_{\hat{\omega}} = \oint \tau \, d\hat{\omega} \qquad (2)$$

Thus, from Eqns (1, 2) follow further observations. When torsion exists, torsion moment M_1 and bimoment B are observed in a bar together. These easy conclusions were strongly confirmed during experiments. Moreover, in zones, where the bimoment is acting, local instabilities of bar walls (waves) are observed - associated with torsion. Beam damage is preceded by it. Intensive bimoment values appear especially in **TWB**s with open **CS**s, see Figure 1C. In bars with thinner walls we observe more intensive waves.

To next more important formulae belong warping functions (3) (or sectorial coordinates), on which depend deplanation, strains and stresses (4,5) in **TWB**s. For open **CS**s can be used definition $(3)_1$. For closed **CS**s should be used definition $(3)_2$, Obrębski [8,9,13].

$$\hat{\omega}(\eta, s) = \int n ds = \omega \, , \quad \hat{\omega}(\eta, s) = \int \left[n - \frac{\tau}{\Theta' G\delta} \right] ds = \omega - \frac{1}{\Theta'} \int_{s_o}^{s} \frac{\tau}{G\delta} ds = \omega - \frac{\Omega}{\oint \frac{\tau ds}{G\delta}} \int_{s_o}^{s} \frac{\tau}{G\delta} ds \quad . \qquad (3)$$

Detailed explanation of these formulae and used notation, see to books Obrębski [8,9,13].

By analytical analysis were applied closed formulae for calculation diagrams of internal forces. Such formulae can be found in many books e.g. Vlasov [19], Rutecki [18], Mutermilch & Kociołek [7], Obrębski [9,13]. The same concern of a longitudinal displacements strains and stresses which can be calculated as follow:

$$u_1 = v_1 - v_2' \eta_2 - v_3' \eta_3 - \Theta' \hat{\omega} \ , \qquad \varepsilon_1 = u_1' = v_1' - v_2'' \eta_2 - v_3'' \eta_3 - \Theta'' \hat{\omega} \ , \qquad (4)$$

$$\sigma_1 = E_1\varepsilon_1 = E_1\left[v_1' - v_2''\eta_2 - v_3''\eta_3 - \Theta''\hat{\omega}\right] \quad , \tag{4}$$

where: u_1 - longitudinal displacement of investigated point, v_i - displacements of bar axis, η_i - coordinates of investigated point, ε_1 - longitudinal strains, σ_1 -normal stresses, E_1 - modified Young's modulus. In any books (see Obrębski [9,13], too), are presented following formulae for calculation of shearing and normal stresses for composite bars, expressed by internal forces:

$$\sigma_1 = \frac{E_1}{E}\left(\frac{T_1}{A} - \frac{M_3\eta_2}{I_3} + \frac{M_2\eta_3}{I_2} + \frac{B\hat{\omega}}{I_{\hat{\omega}}}\right) \quad \tau_{1s} = \tau_O - \frac{1}{\delta}\left(\frac{T_2\tilde{S}_3}{I_3} + \frac{T_3\tilde{S}_2}{I_2} + \frac{M_{\hat{\omega}}\tilde{S}_{\hat{\omega}}}{I_{\hat{\omega}}}\right), \tag{5}$$

Moreover, it is proposed to be applied additionally Huber-Mises-Hencky hypothesis, similarly as in many standards, including Polish for steel structures.

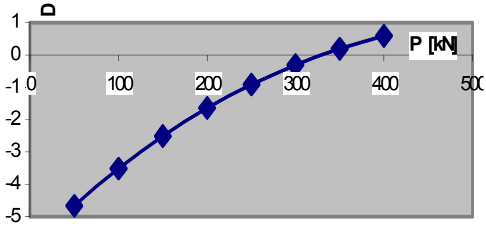

Figure 4: Example of diagram D obtained from Equation (6) for simple compressed bar

In the papers [12,17] Obrębski has expressed an opinion that the most general, and efficient criterion for evaluation of critical loading is a comparison to zero of the main determinant of a set of equations describing equilibrium of the whole structure:

$$D = \det\left[K(P,\omega,v,a,M,m,d,t)\right] \quad . \tag{6}$$

where: P – system of one or more forces, ω – frequency of free vibrations, v – loading velocity, a –acceleration of loadings, M –moving mass, m –mass of structure, d – dumping conditions, t –time etc. Many examples of application of such criterion were presented by Obrębski with co-workers in [9,12-17]. So, can be solved multiparametrical instability problems (6) with critical lines (Figure 4) or surfaces Obrębski [17], with J.Tolksdorf, too.

5. Own experiments

There, were performed numerous experiments, which are very shortly introduced below.

5.1. The author's own experiments for cantilever beam

There, was investigated cantilever beams behaviour under bending-torsion loading with schemes given in Figures 1,2. As specimens were used natural scale brazen **TWB**s with approximate dimensions 10x20x196cm, with wall thicknesses 0.5mm, 1.5mm and 2.5mm. Strains in two **CS**s β-β, displacements in **CS**s α-α and load capacity of the bar were measured. Moreover, the behaviour of the beam was observed and documented carefully.

There, 17 bars were investigated. Out of these, 13 with a vertical position (as in Figures 1-4,5) and rectangular **CS** (with Urbaniak [10,17]) and 4 with a horizontal orientation (together with Flont [1]). In all of the above experiments, before bar damage (breaking) some waves appeared at the fixed end (Figure 1C, 6) on both bar sides and in the bottom wall. Some waves appear at loaded bar end, too, where longitudinal displacements were constrained by a rigid cork, Figure 1C. Development of waves during this type of experiments is shown on diagrams in the Figure 2b.

a)

b)

c)
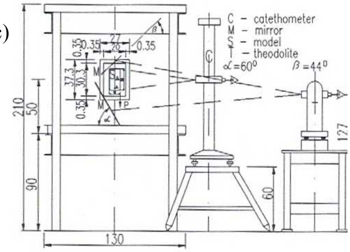

Figure 5: View on stand for bending-torsion loading of rectangular brazen cantilevers a); four steel frames for measurements of displacements; at left fastening and hinge (breaking point) b); a) Scheme of optical observation for circuital and longitudinal displacements c)

In the Figure 6d are compared four similar bars with identical wall thickness. Two of the bars have an open **CS** and the opposite loaded end is totally free, or constrained by a cork. Similarly, the other two bars with a closed **CS** have the opposite end free or constrained by a cork, too. The different distances of breaking from the fixed end on the bottom wall and its inclination are interesting, Figure 6a-d. Here we should remember that for open type **CS**s, warping stresses are much higher. Also, the distribution of normal longitudinal stresses for bars with open and closed **CS**s is dramatically different.

a)
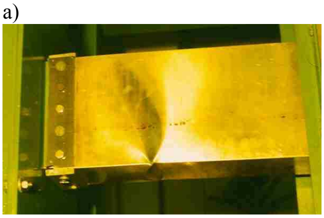
b)

c)

d)


Figure 6: View of hinge (breaking point) of cantilever beams with planarly constrained fixed end a); waves on lower wall and on both sides of the bar b,c); four cases of bars (Figure 1A) seen from down (wall thickness δ=0.5mm) d)

5.2. Bar loaded by pure bimoment

In this type of experiments, the short bar was loaded by pure bimoment only, Figures 7,8. As the scheme in Figure 7a shows, pure bimoment was applied at the bottom end of the bar. At the top of the specimen, in each case a rigid cork was applied to constrain longitudinal displacements and to stiffen the whole model, Figures 7b, 8. Also, three different types of longitudinal slits were applied: in the middle, in one quarter of the wider wall and in the bar corner, Figure 8. Moreover, three wall thicknesses were applied: 0.5mm, 1.0mm, 1.5mm.

Waves appeared along the slit, Figure 8, at a certain value of bar loading *P* (Figure 7a). The value of force P when waves appeared, was noted as critical loading by bimoment B. Beside slit edge waving, certain rotations of the top end of the bars were observed. So, when bimoment is applied, torsion appears. In this series of experiments, without any doubt, waves and critical loading were the result of pure bimoment application, only. So, it all confirms the thesis that bimoment is significantly responsible for wavy effects on side walls and along slits, too Fig.4a.

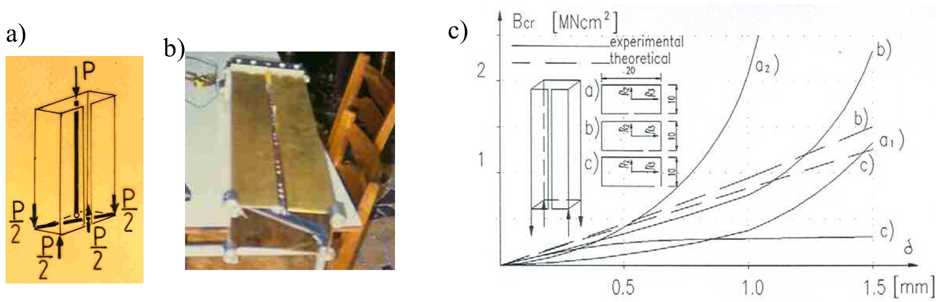

Figure 7: Scheme of measurements of critical bimoment a); with displacements planarly constrained by strong steel cork at top b); loading system by pure bimoment at bottom bar end a,b); diagrams of measured and calculated critical bimoments c)

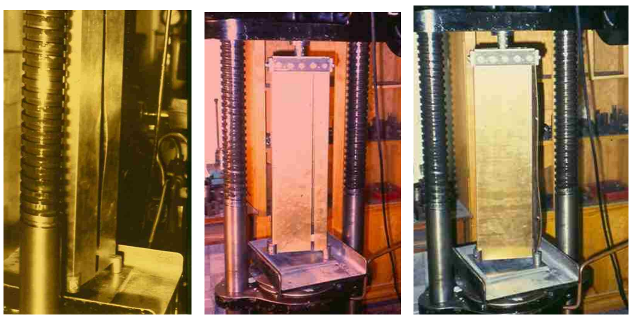

Figure 8: Visible three different wave types at free longitudinal edges for bars with longitudinal slit in three positions of wider wall.

5.3. Investigations of simple thin-walled frames

The problem of computer analysis of space frames taking into consideration of bimoments, too, was numerically investigated by some authors. There, can be mentioned e.g. works by J.Rutecki [18], J.H.Argyris and D.Radaj (1971), R.Dziewolski (IASS, Kielce 1973), Obrębski [8,9,13,15,17] (1985, 1991), K.Grygierek (Ph.D. dissertation, Gliwice, 2003), and C.Szymczak et al. (2003). There, still is serious question about real behaviour of space bar frames. Therefore, N. Jankowska in she's Ph.D. dissertation [2] (supervised by J.B.Obrębski), has investigated 8 models of simple thin-walled frames, type L, T and Y, Figures 3,9,17,18. The frames were composed of the 2 or 3 **TWB**s, made of the brass, connected with one central node, only. By both ends of each bar, in distance of 2.5 cm were glued 25 electro-resistance rosettes. There was applied very modern in that time electronic bridge of the firm VISHAY, system 5000, Figure 3c. All together, were investigated 32 **CS**s, in it most of them placed by central node.

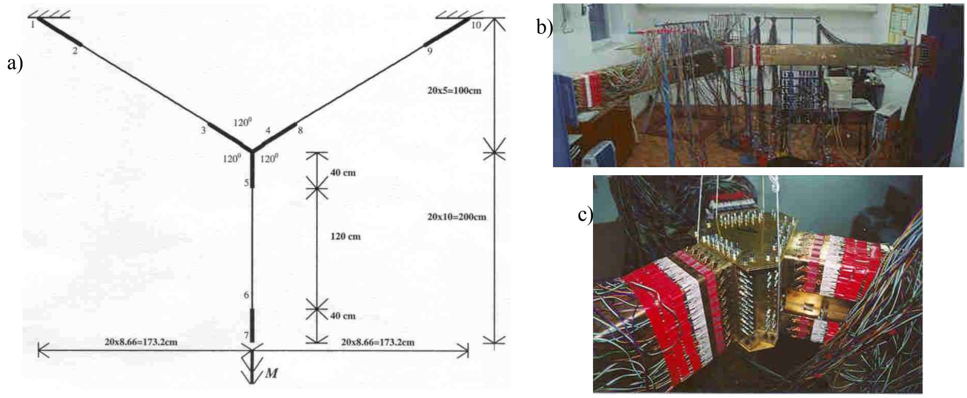

Figure 9: Scheme of frame type Y a); general view b); node of the frame c) Jankowska [2]

6. Applied models for numerical analyses of investigated cantilever bars

For the reason of parallel investigations by experiment, analytically and numerically by FEM (program ROBOT v.16), were applied three different procedures for describe and next to analyze the same physical model.

6.1. Model and analytical solutions

There, were calculated from theoretical formulae derived for straight **TWB**s, all geometrical characteristics of bar **CS**s, and internal forces, displacements and stresses.

6.2. Model and numerical solution by Finite Element Method

The bar was divided on rectangular shell elements with approximate dimensions 2×2cm by **CS**s β-β on distance 6 and 8cm (Figure 1). Remaining part was divided on approximate shell elements 2×5cm. Next, by MS Excel were obtained stresses in the same points as by experimental and analytical approaches with distance 1cm between each the other.

6.3. Elaboration of experimental results

Strains were measured experimentally by electro-resistance method. Then were calculated: a) bimoment B and bending-torsional moment M_ω , shown in the Figure 13 (method proposed by Obrębski [17]); b) by MS Excel were calculated geometrical characteristics of **CS**s, normal stresses, shearing stresses, principal strains and stresses, angle of shape deformation. Some selected results are presented in the Figures 10,11,13,14.

Internal Force	Model 21 with open cross-section		Model 22 with closed cross-section	
	analytical	measured	analytical	Measured
B [$kNcm^2$]	831.82	848.475	-4.826	9.65
M_ω [kNcm]	-10.1908	-2.175	2.189	3.35

Figure 10: Calculated analytically and measured bimoments and bending-torsion moments; measured forces were calculated according to formulae $(1)_2$ and $(2)_2$

7. Comparisons of obtained results

Results of all three types of experiments were compared with theoretical and even with obtained by FEM, too. Some selected, more important results are presented below.

7.1. Comparisons for thin-walled bars loaded by pure bimoment

As it is visible in the Figure 9, the value of force P when waves appeared was noted as critical loading by bimoment B calculated according to formula (1c). The experimental results obtained are compared in Figure 7c, with similar ones calculated analytically by means of theoretical formulae derived by Obrębski in the book [13]. For thinner bar walls, the convergence is good enough. Experimental curves show high nonlinearity of the phenomenon and for thicker **CS**s are much higher. On the contrary, there we observe that theoretical values of B_{cr} depend almost linearly on the thickness of bar walls. In any case it is important that the bimoment has its critical value and can be calculated!

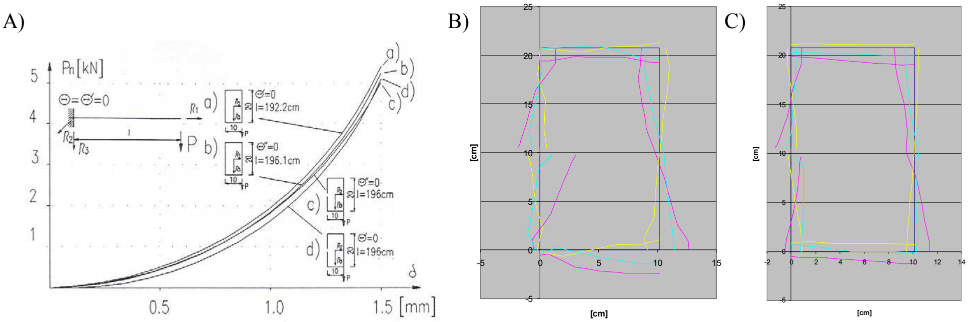

Figure 11: Diagrams of P_n dependent on wall thickness δ A); Diagrams of strains (black lines – shape of **CS**, red – longitudinal, yellow – cirquital , green – inclined) in **CS** β-β: 2cm from fastening B) 55 cm from fastening c)

7.2. Some comparative results for series of ten thin-walled cantilevers

As the first, in the Figures 11,12 are shown curves evaluating load capacity of the four similar cantilevers. There, values of maximal loads for bars with walls thickness δ=0.5 mm were measured (Figure 12), and for models with δ=1.5 mm, approximately estimated (quicker deflections to frames). Character of all curves is strongly nonlinear. There, the bar with the open **CS** obtains a load capacity of 45.143kg (with rigid cork at free bar end $\Theta' = 0$) higher than that of the bar with a closed **CS**, 43.883kg (with $\Theta'' = 0$ at free bar end). Moreover, by thicker bar walls, the influence of local instability is much smaller.

Scheme of the cantilever	P_n load capacity [N] (hanging mass [kg]) by given bar cross-section δ=0.5 mm			
	Open cross-section 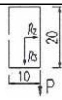		Closed cross-section 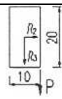	
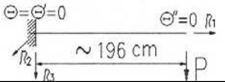	Model nr 1	302.858N (~30.883kg) >25.833kg	Model nr 4 Model nr 6	430.345N (43.883kg) 45.723kg
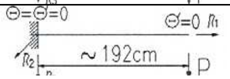	Model nr8 Model nr 2	442.702N (~45.143kg) >40,117kg 35,833kg	Model nr 5	488.793N (49.843kg)

Figure 12: Maximal loadings (load carrying capacity) for bars fastened at left and with open or closed **CS**s, with free- or planarly constrained right end

It is worthy to pointing, that after electro-resistance measurements of strains, normal and shearing stresses were calculated. Next applying formulae $(1)_2$ and $(2)_2$ were estimated values of bimoments B and bending-torsion moments, shown in the Figure 10. It is well visible high convergence of analytical and measured values for open **CS**s. Absolute value of an error in all cases is almost identical.

MODEL	Bondary conditions at bar end	Value	η=2cm				η=55cm			
			σ_x kN/cm^2	σ_s kN/cm^2	τ_{xs} kN/cm^2	γ_{xs} degrees	σ_x kN/cm^2	σ_s kN/cm^2	τ_{xs} kN/cm^2	γ_{xs} degrees
NR 11 open	$\Theta''=0$	Maximum	6,665489	3,110425	2,346317	**0,032172**	3,672981	0,420722	1,430033	0,019608
		Minimum	-8,44217	-2,1735	-2,0864	-0,02861	-4,96572	-2,33927	-1,47828	**-0,02027**
NR 12 closed	$\Theta''=0$	Maximum	4,953299	4,862757	0,909355	0,012469	3,80453	0,680318	2,068891	**0,028368**
		Minimum	-5,25081	-1,4889	-2,51783	**-0,03452**	-3,49994	-1,02846	-0,90461	-0,0124
NR 13 open	$\Theta'=0$	Maximum	8,668617	4,4907	0,542219	0,007435	3,226324	0,408864	2,000116	0,027425
		Minimum	-2,47904	0	-1,68369	-0,02309	-3,37746	-0,72747	-0,51173	-0,00702
NR 14 closed	$\Theta'=0$	Maximum	4,659106	1,715113	-0,98822	0,012237	4,390422	1,462034	0,588788	0,008073
		Minimum	-4,75694	-0,71898	-0,98822	-0,01355	-2,81556	0,183384	-0,62834	-0,00862

Figure 13: Experimental data: σ_x - longitudinal normal stresses, σ_s - cirquital normal stresses, τ_{xs} shearing stresses, γ_{xs} - angle of shape deformation

MODEL	Bondary conditions at bar end	Value	η=2cm			η=55cm		
			σ_1-princ. kN/cm^2	σ_2-princ. kN/cm^2	Angle φ_n degrees	σ_1-princ. kN/cm^2	σ_2-princ. kN/cm^2	Angle φ_n Degrees
NR 11 open	$\Theta''=0$	Maximum	6,790865	1,912319	44,32515	3,672981	1,66E-16	44,92024
		Minimum	-1,08602	-8,44217	-42,896	-0,68297	-4,96791	-43,6244
NR 12 closed	$\Theta''=0$	Maximum	5,904744	0,964992	43,37957	3,809741	0,573367	40,0305
		Minimum	-1,45381	-4,2006	-39,939	-0,1963	-3,51591	-40,8167
NR 13 open	$\Theta'=0$	Maximum	8,747777	4,357532	29,46239	3,226324	0,113579	44,57245
		Minimum	0	-2,51019	-31,4046	-0,39569	-3,37746	-44,6412
NR 14 closed	$\Theta'=0$	Maximum	4,692641	1,681578	42,42039	4,532361	1,436232	42,67831
		Minimum	-0,67767	-4,76033	-43,2355	-1,62445	-5,48792	-38,4142

Figure 14: Experimental data: principal stresses σ_1, σ_2 and φ_n - angle of its inclination

MODEL	Bondary conditions at bar end	Value	η=2cm				η=55cm			
			σ_x kN/cm²	%	τ_{xs} kN/cm²	%	σ_x kN/cm²	%	τ_{xs} kN/cm²	%
NR 11 Open	$\Theta'' = 0$	Maximum	5,806991	87,12	0,007393	0,31	4,3187685	117,58	0,000713	0,049
		Minimum	-5,99928	71,06	-0,00652	0,31	-4,45941	89,80	-0,0007	0,047
NR 12 closed	$\Theta'' = 0$	Maximum	4,207309	84,93	0,004851	0,53	3,125967	82,16	0,000804	0,038
		Minimum	-4,20777	80,13	-0,00485	0,19	-3,125963	89,31	-0,00081	0,089
NR 13 open	$\Theta' = 0$	Maximum	5,128760	59,16	0,005674	1,05	3.377746	95,52	0,000729	0,03
		Minimum	-5,128722	206,88	-0.00479	0,28	-3,377727	89,42	-0,000730	0,14
NR 14 closed	$\Theta' = 0$	Maximum	4,325001	92,82	0,00493	-0,49	3,025298	68,91	0,000761	0,13
		Minimum	-4,32452	90,91	-0,004932	0,49	-3,02493	93,08	-0,000765	0,12

Figure 15: Results of calculation by FEM – by means of program ROBOT v.16

7.3. Some results and its evaluation for series of thin-walled frames

Jankowska [2] has presented proper diagrams of shearing and normal stresses (e.g. Figure 17b), and calculated among the other, internal forces, associated with torsion: B – mimoment and $M_{\hat{\omega}}$ - bending-torsion moment, according to formulae (1), by method proposed by J.B.Obrębski. Some results are given in the Figure 18. So, the transmission of bimoment through node (from 16,57% to 33,35) and its dependence on node rigidity was confirmed. It is important, that similar observation concerning of bimoments transmission, obtained numerically by super-elements technique, was reported by C.Szymczak et al., too.

MODEL	Bondary conditions at bar end	Value	η=2cm				η=55cm			
			σ_x kN/cm²	%	τ_{xs} kN/cm²	%	σ_x kN/cm²	%	τ_{xs} kN/cm²	%
NR 11 open	$\Theta'' = 0$	Maximum	6,147748	92,23	0,352287	15,01447	4,373496	119,07	0,341685	23,89
		Minimum	-6,16339	73,01	-0,10737	5,146185	-4,38435	88,29	-0,10077	6,81
NR 12 closed	$\Theta'' = 0$	Maximum	6,611549	133,47	0,371427	40,8451	3,341825	87,83	0,227769	11,01
		Minimum	-6,53584	124,47	-0,50132	19,9108	-3,30866	94,53	-0,20468	22,62
NR 13 open	$\Theta' = 0$	Maximum	5,288191	61,00	0,362693	66,8905	3,483471	107,97	0,352032	17,60
		Minimum	-5,28597	213,22	-0,11355	6,744116	-3,47785	102,97	-0,10714	20,93
NR 14 closed	$\Theta' = 0$	Maximum	6,764159	145,18	0,882758	-89,3281	3,67692	83,74	0,448513	76,17
		Minimum	-6,67099	140,24	-2,20E-07	2,23E-05	-3,4254	121,65	-2,10E-07	3,34E-05

Figure 16: Results of analytical approach executed by means of MS Excel

7. Final remarks

The more important conclusions are listed below. For wider information and literature, please, see to author's paper [17]. Bimoment is as well real an internal force as: longitudinal force, shearing force, bending and torsion moments, and can be calculated their critical values including combined loadings. Bimoment can be measured experimentally, especially for open **CS**s. In torsioned bars always appears together – bimoment, bending-torsion moment and torsion moment. Any type of loading and combined loading can lead to the critical state of bar behaviour. The cirquital normal stresses for **TWB**s can reach up to (0-98.17%, η=2cm) and (11.4-47,1%, η=55cm) of longitudinal normal stresses (see Figure 17). Similarly, the shearing stresses for **TWB**s can reach up to (6.25 ÷ 67.92%, η=2cm) and (13.41 ÷ 61.99%, η=55cm) of longitudinal normal stresses (see Figure 17). In investigated cantilevers the angles of shape deformation (non-dilatation strain) for open

CSs reach up to -0,034^0 and for closed **CS**s +0.032^0 (93,20% when η=2cm or 71,45% when η=55cm - of similar angles for closed **CS**s, Figure 13). In Vlasov's theory [19] it was assumed zero! □ The analytically obtained stresses were for cantilever bars close to experimental ones, than similar calculated by FEM (see Figures 13,15,16). □ Calculation of critical forces is possible for composite bars, under combined loading, too [9,12,13,15,17]. □ Many effects observed in behaviour of **TWB**s, taken under consideration in standards by means of certain coefficients, can be calculated simply by author's theory. □ Assumptions and possibilities of theory of **TWB**s elaborated by Obrębski [8,9,13,17] seems to be well confirmed by experiments, much more better than in the others mentioned in this paper, too. □ So, computer algorithms together with good theory, are giving the best solutions.

In this paper only the more important remarks and conclusions are presented. It should be pointed out that nowadays, in standards, torsion and bimoment are almost completely neglected. There is a strong tendency to eliminate stresses calculation from the dimensioning process. It seems to be highly dangerous. **Investigations are continued.**

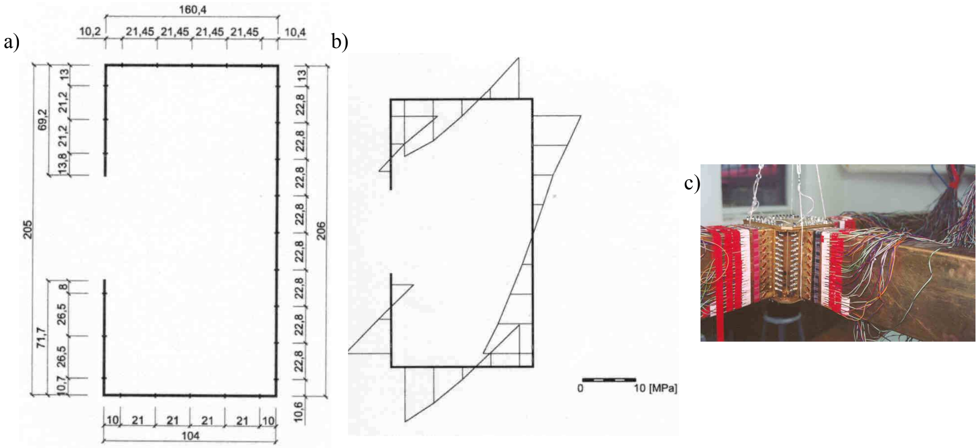

Figure 17: Location of rosettes in one of the **CS**s a); diagram of measured normal stresses [2] b); node of frame type T with sensors for electro-resistance measurements c)

I – number of sheets in central node	Frame type Li				Frame type Ti						Frame Yi			
	i=1		i=2	i=3	i=1		i=2		i=3		i=1		i=2	
	L1	%	L2	L3	T1	%	T2	%	T3	%	Y1	%	Y2	%
C –active CS	-1364		-1355	-1259	-1495		-1390		-1339		-1413	22,79	-1333	
B-passive CS	-455	33,35			-285	19.06	-261	18,77	-241	17,99	-322	22,79	-285	21,38
E-passive CS					287	19.19	244	17,55	222	16,57	259	18,33	223	16,73

Figure 18: Measured bimoments (Jankowska [2])

References

[1] Flont P., *Badania doświadczalne stanu odkształcenia i naprężenia pewnej klasy prętów cienkościennych.* (M.Sc. dissertation – supervisor J.B. Obrębski). Warsaw University of Technology, Warsaw, 1995.

[2] Jankowska N., *Influence of nodes deformations on internal forces in thin-walled frames*. (In Polish, doctor dissertation – supervisor J.B.Obrębski), Warsaw University of Technology, Warsaw 2006.

[3] Jastrzębski P., Mutermilch J., Orłowski W., *Strength of Materials* (In Polish), Arkady, 1985 (Vol.1), 1986 (Vol.2).

[4] Kollbrunner C.F., Hajdin N., *Dünnwandige Stäbe*. T. 1,2. Berlin, Heidelberg, New York, Springer, 1975.

[5] Magnucki K., Szyc W., *Structures with Thin-Walled Open CSs* (In Polish). Publ.House of Wyższej Szkoły Pedagogicznej im. T.Kotarbińskiego w Zielonej Górze, 1997.

[6] Murray N.W., *Introduction to the Theory of Thin-Walled Struct*. Oxford Eng.Sc. Ser., 1984

[7] Mutermilch J., Kociolek A., *Strength and Stability of Thin-Walled Bars with Open Cross-Sections* (In Polish), Warsaw, WPW, 1972.

[8] Obrębski J.B., Second-order and second-approximation theory in the statics and dynamics of thin-walled straight bars. *Journal of the Thin-Walled Structures*, Appl.Sc.Publ. 8,1989; 81-97.

[9] Obrębski J.B., *Thin-Walled Elastic Straight Bars* (In Polish). WPW,(lect. notes), Warsaw 1991; pp.452.

[10] Obrębski J.B., Urbaniak Z., El-Awady M.E., On designing of the thin-walled bars in the light of theory and experiments, in *Int. IMEKO-GESA Symp. on Risk Minimisation by Experimental Mechanics*, 1992, Düsseldorf, FRG.

[11] Obrębski J.B., Experimental estimation of bimoment and bending-torsional moment (In Polish), in *XVI Symp.on Experim.Mech. of Solids,*Jachranka,Poland,1994;249-252.

[12] Obrębski J.B., Uniform criterion for geometrical unchengeability and for instability of struc tures, in *Proc. of the International Conf.on Stability of Structures*. Zakopane, Poland, 1997.

[13] Obrębski J.B., *Strength of Materials* (In Polish, lecture notes of Warsaw Univ.of Techn.), Micro-Publisher J.B.Obrębski Wydawn.Naukowe, Printed by AGAT,Warsaw 1997, pp.238.

[14] Obrębski J.B., Szmit R., Dynamics and dynamical stability of tall buildings, (Invited lecture). Int.Conf. ICSSD, Taipei, Taiwan, 2000, 85-94.

[15] Obrębski J.B., On the mechanics and strength analysis of composite structures. (Invited paper), in *SEMC*, Cape Town, 2-4.04.2001, A.Zingoni (ed.), Elsevier Sc. Ltd., Amsterdam-(..), 2001, 161-172.

[16] Obrębski J.B., Advantages of 3D-Time Space Description for dynamical analysis of structures,(Invited paper),in *Int.Conf.IASS-APCS*,Taipei,Taiwan,2003,40-41+CD-ROM.

[17] Obrębski J.B., Review of own complex researches related to bar structures, in *XIV LSCE - Lightweight Structures in Civil Engineering - Contemporary Problems*, Local Seminar of IASS Polish Chapter, Warsaw, 5 December, 2008, 87-128.

[18] Rutecki J., *Strength of Thin-Walled Structures* (In Polish), Warsaw, PWN, 1957.

[19] Vlasov V.Z., Thin-walled elastic bars (In Russian), Moscow, 1940, 1959.